Copy
RM L9F08

RESEARCH MEMORANDUM

AERODYNAMIC CHARACTERISTICS OF AN AIRFOIL-FOREBODY SWEPT FLYING-BOAT HULL WITH A WING AND TAIL SWEPT BACK 51.3° AT THE LEADING EDGE

By Rodger L. Naeseth and Richard G. MacLeod

Langley Aeronautical Laboratory
Langley Air Force Base, Va.

NATIONAL ADVISORY COMMITTEE
FOR AERONAUTICS

WASHINGTON
September 9, 1949

NACA RM L9F08

NATIONAL ADVISORY COMMITTEE FOR AERONAUTICS

RESEARCH MEMORANDUM

AERODYNAMIC CHARACTERISTICS OF AN AIRFOIL-FOREBODY SWEPT FLYING-BOAT HULL WITH A WING AND TAIL SWEPT BACK 51.3° AT THE LEADING EDGE

By Rodger L. Naeseth and Richard G. MacLeod

SUMMARY

An investigation was made at low speeds to determine the aerodynamic characteristics of an airfoil-forebody swept flying-boat hull with a wing and tail swept back 51.3° at the leading edge. The hull was derived by sweeping aft the water planes above the chines of a deep-step flying-boat hull of a previous investigation.

The results of the investigation indicated that the swept hull had a minimum drag coefficient about the same as the parent model or a streamline body after accounting for the difference in interference effects of the support wings. The minimum drag coefficient for the swept hull including the interference effects of the 51.3° swept-back wing was 0.0038.

The use of wing leading-edge flaps or leading-edge droop with fence on the wing-hull-tail combination gave a stable configuration.

The deflection of split or extensible split wing flaps on the wing-hull-tail combination with wing stall-control devices deflected gave a more linear variation of pitching-moment coefficient with lift coefficient; however, only the extensible split flaps were effective in increasing the maximum lift coefficient.

INTRODUCTION

Because of the requirements for increased range and speed in flying boats, an investigation of the aerodynamic characteristics of flying-boat hulls as affected by hull dimensions and hull shape is being conducted at the Langley Laboratory. Results of several phases of the investigation are given in references 1 to 3.

Tests of refined deep-step planing-tail flying-boat hulls (reference 3) indicated that these hulls have drag values comparable with those of landplane fuselages but retain acceptable hydrodynamic performance (reference 4). The hull volume, however, is less than the landplane fuselage volume and most of the volume is located forward of the wing. Thus a balance problem is encountered in placing most types of pay load because the relationship of the wing and step to the center of gravity must be maintained for aerodynamic and hydrodynamic reasons. A possible solution to the balance problem was to move the volume aft. A new hull was derived from Langley tank model 237-7B, the volume of which was shifted aft with respect to the center of gravity by sweeping aft the water planes above the chines. The new hull has been designated Langley tank model 237-6SB and is called the swept hull.

In keeping with present trends in high-speed aircraft, a wing swept back 51.3° at the leading edge was used instead of the straight support wings used in previous investigations. This paper presents results of tests of the swept-hull-wing combination and wing alone to determine the aerodynamic characteristics of the hull including the effects of wing interference for comparison with the characteristics of the parent model (reference 3) and tests of the hull with sweptback wing and tail in conjunction with various high-lift and stall-control devices to provide data for design of dynamic tank models using sweptback wings.

Results of tank tests (reference 5) indicate that the swept hull will probably give satisfactory hydrodynamic performance.

COEFFICIENTS AND SYMBOLS

The results of the tests are presented as standard NACA coefficients of forces and moments. Rolling-moment, yawing-moment, and pitching-moment coefficients are given about the 30-percent-wing-mean-aerodynamic-chord point shown in figure 1.

The data are referred to the stability axes, which are a system of axes having their origin at the center of moments shown in figure 1 and in which the Z-axis is in the plane of symmetry and perpendicular to the relative wind, the X-axis is in the plane of symmetry and perpendicular to the Z-axis, and the Y-axis is perpendicular to the plane of symmetry. The positive directions of the stability axes are shown in figure 2. The coefficients and symbols are defined as follows:

C_L lift coefficient (Lift/qS)

C_D drag coefficient (Drag/qS)

[redacted]

C_Y lateral-force coefficient (Y/qS)

C_l rolling-moment coefficient (L/qSb)

C_m pitching-moment coefficient ($M/qS\bar{c}$)

C_n yawing-moment coefficient (N/qSb)

Lift = -Z

Drag = -X, when $\psi = 0^\circ$

X force along X-axis, pounds

Y force along Y-axis, pounds

Z force along Z-axis, pounds

L rolling moment, foot-pounds

M pitching moment, foot-pounds

N yawing moment, foot-pounds

q free-stream dynamic pressure, pounds per square foot $\left(\frac{1}{2}\rho V^2\right)$

S wing area, 5.73 square feet

$\bar{c}$ wing mean aerodynamic chord, 1.424 feet $\left(\frac{2}{S}\int_0^{b/2} c^2 dy\right)$

c local wing chord, feet

b wing span, 4.22 feet

V free-stream velocity, feet per second

ρ mass density of air, slugs per cubic foot

α angle of attack of chord line measured in plane of symmetry, degrees

α_h angle of attack of hull base line, degrees

[redacted]

ψ angle of yaw, degrees

i_t angle of stabilizer with respect to wing root chord line, degrees

R Reynolds number based on wing mean aerodynamic chord

$C_{m_\alpha} = \frac{\partial C_m}{\partial \alpha}$

$C_{n_\psi} = \frac{\partial C_n}{\partial \psi}$

$C_{Y_\psi} = \frac{\partial C_Y}{\partial \psi}$

$C_{l_\psi} = \frac{\partial C_l}{\partial \psi}$

$C_{m_{i_t}}$ effectiveness of the tail at $C_L = 0$ $\left(\frac{\partial C_m}{\partial i_t}\right)$

MODEL

The general arrangement of the model is shown in figure 1 and a photograph of the model on the support struts, in figure 3.

The hull, Langley tank model 237-6SB, (fig. 1 and table I) was designed by the Hydrodynamics Division and the Stability Research Division of the Langley Laboratory and was essentially Langley tank model 237-7B (reference 3) with water planes above the chines shifted aft and modified to give the side elevation shown in figure 1. The length-to-beam ratio was about 6 for the swept hull. The hull used in the aerodynamic tests was a tank dynamic model of the usual balsa and tissue construction. The volume and the areas of the hull were: volume, 1447 cubic inches; surface area, 1101 square inches; frontal area, 56.8 square inches; side area, 418 square inches.

The wing was positioned with the 0.30 mean aerodynamic chord at the mean of the useful center-of-gravity range set by hydrodynamic design. The overhang of the leading edge of the wing is due to the shape of the hull and the large root chord of the swept wing which was

adapted to the original straight-wing hull design. Though not included in these tests, it was thought that an inboard jet installation or wing-root fairings would alleviate the structural problem.

The wing and tail (fig. 1) were constructed of mahogany, had NACA 65_1-012 sections parallel to the plane of symmetry, and were swept back 51.3° measured at the leading edge. The wing had zero geometric dihedral; the horizontal tail was set at 15° geometric dihedral. The wing aspect ratio was 3.11; taper ratio, 0.50; and area, 5.73 square feet. Horizontal-tail area was 0.97 square feet and vertical-tail area was 0.61 square feet.

The leading-edge flaps, leading-edge droop, fence, split flaps, and extensible split flaps are detailed in figure 4.

The leading-edge flaps and droop were similar to those reported in references 6 and 7, respectively. The $0.465\frac{b}{2}$ leading-edge flaps (fig. 4(a)) were of constant chord with the inboard end located at $0.445\frac{b}{2}$. The angle of the flap chord with respect to the wing-chord plane, measured in a plane normal to the wing leading edge, was 50°.

The leading-edge droop (fig. 4(b)) covered a span of $0.487\frac{b}{2}$ with the inboard end located at $0.438\frac{b}{2}$. The chord of the drooped portion of the wing was 0.14 local wing chord on the upper surface and 0.16 local wing chord on the lower surface. The leading edge was drooped 50° about the 0.16 chord line, measured in a plane normal to the 0.16 chord line. The gaps along the upper-surface 0.14 chord formed by drooping the leading edges were filled; the gaps at the inboard and outboard ends of the drooped section were not filled except for one test. The fence used in conjunction with the droop nose and the leading-edge flap for some tests (fig. 4(b)) was of constant height, 0.65 maximum local wing thickness, and was located at $0.513\frac{b}{2}$.

The $0.487\frac{b}{2}$ split flaps (fig. 4(c)) had a chord equal to 30 percent of the local wing chord. The inboard end of the flaps was located at $0.198\frac{b}{2}$. The flaps were deflected 40° from the wing surface measured in a plane normal to the hinge line.

The extensible split flaps were the same flaps as the split flaps but were moved aft as shown in figure 4(d). The flap deflection was 31° measured with reference to the wing-chord plane in a plane normal to the hinge line.

[redacted]

TESTS

Test Conditions

The tests were made in the Langley 300 MPH 7- by 10-foot tunnel. Tests to determine the aerodynamic characteristics of the hull were made at a dynamic pressure of 100 pounds per square foot. The stability tests of the complete configuration were made at the lower dynamic pressure of 9.4 pounds per square foot so that the angle-of-attack range could be extended through the stall without overloading the hull. Corresponding air velocities were 209 and 61 miles per hour. Reynolds numbers for these airspeeds, based on the mean aerodynamic chord of the model (1.424 ft), were 2.6×10^6 and 0.8×10^6, respectively; corresponding Mach numbers were 0.27 and 0.08.

Corrections

Blocking and buoyancy corrections have been applied to the data. The angles of attack, the drag coefficients, and the tail-on pitching-moment coefficients have been corrected for jet-boundary effects.

No corrections have been applied to the data to account for model-support-strut tares.

Test Procedure

The aerodynamic characteristics of the hull, including the interference of the 51.3° sweptback support wing, were determined by testing the wing alone and the wing-and-hull combination under the same conditions. The hull aerodynamic coefficients were thus determined by subtraction of wing-alone coefficients from wing-and-hull coefficients. In order to minimize possible errors from transition shift, transition was fixed on the wing and hull by means of roughness consisting of carborundum particles of approximately 0.008-inch diameter. Roughness was applied to the wing for a length of 8 percent local airfoil chord measured along the airfoil contours from the leading edge on both upper and lower surfaces. Hull transition was fixed by a $\frac{1}{2}$-inch strip of carborundum particles located 8 percent of the hull length aft of the leading edge of the hull measured parallel to the base line.

Longitudinal-stability tests were made of the complete model (wing-hull-tail) with various high-lift and stall-control devices. Lateral-stability derivatives were obtained for the complete model configuration with nose flap deflected from tests through the angle-of-attack range

at ±5° yaw. Tests were made through an extended yaw range at 10.5° angle of attack with and without leading-edge flaps. Transition was not fixed on the hull or the wing for the complete-model tests or for the plain-wing-alone tests presented for comparison.

RESULTS AND DISCUSSION

The aerodynamic characteristics in pitch of the swept hull, including the interference effects of the 51.3° sweptback wing, are presented in figure 5. Figures 6, 7, and 8 present the characteristics in pitch of the complete configuration (wing-hull-tail) with leading-edge and trailing-edge devices. The variation with lift coefficient of the lateral-stability derivatives for the complete-model configuration with leading-edge flap is given in figure 9; characteristics in yaw are presented in figure 10.

Hull

Drag characteristics.- The data of figure 5 indicate that for a Reynolds number of about 2.6×10^6 the swept hull, Langley tank model 237-6SB, had a minimum drag coefficient of 0.0038 including the interference of the 51.3° sweptback support wing.

Although the wing loadings of the swept-hull combination and the parent combination (Langley tank model 237-7B) were about the same, a direct comparison could not be made because of the difference in wing interference resulting from the small amount of wing enclosed in the swept-hull combination as compared to the parent combination. A discussion of wing interference is given in reference 8 for conventional hulls. Similar unpublished work on the effects of wing interference on the aerodynamic characteristics of hulls of the 237-series, not including the swept hull, gives the increment of drag due to wing interference for hulls similar to the swept hull. After accounting for the difference in wing interference by means of this increment, the minimum drag coefficient of the swept hull is thought to be about the same as that of the parent hull. The parent hull had a minimum drag coefficient comparable to a streamline body. The range of angles of attack of the hull base line for minimum drag was 4° to 6° and was slightly higher than previously tested deep-step hulls (reference 3).

Longitudinal stability characteristics.- The value of the parameter C_{m_α} was −0.0014, which indicated that the hull with wing interference had a slight amount of longitudinal stability.

[redacted]

Wing–Hull–Tail Combinations

Lift characteristics.– The plain wing alone (fig. 6), had a lift-curve slope of 0.055 and a maximum lift coefficient of 1.08. The complete configuration with leading-edge flaps and fences or with leading-edge droop and fences gave a maximum lift coefficient of about 1.34. Removal of the fences from the complete configuration with leading-edge flaps reduced the maximum lift coefficient to 1.25. Lift flaps added to these configurations (fig. 7) generally decreased the angle of zero lift from about 1° to −4° but had little effect on the maximum lift values except in the case of the configuration of the extensible split flap and the leading-edge flap which had a maximum lift coefficient of 1.65. Based on the area of the wing plus the area of the extended flap, the maximum lift coefficient is 1.50. Thus, it appears that approximately 40 percent of the increase in maximum lift coefficient may be attributed to the increase in total wing area.

Fairing the gaps at the inboard and outboard ends of the leading-edge droop (fig. 7) increased the maximum lift coefficient slightly.

Longitudinal stability characteristics.– The plain wing alone (fig. 6) was unstable throughout the lift range. The use of leading-edge flaps or droop with fence on the complete configuration resulted in generally stable slopes. The leading-edge-droop-and-fence configuration had the most stable and linear pitching-moment curve. Removal of the fence from the leading-edge-flap configuration resulted in little change in stability in the low lift range but produced neutral stability in the 0.6 to 0.8 lift-coefficient range.

The data of figure 7 indicate that the combination of lift flaps and stall-control devices on the complete configuration gave a slight increase in stability and more linear pitching-moment curves.

The strong effect of the tail in producing stability through the stall is indicated by the data presented in figure 8. Effectiveness of the tail as measured by $C_{m_{i_t}}$ was −0.014 at $C_L = 0$.

Lateral stability characteristics.– The parameter C_{n_ψ} (fig. 9) indicates that the directional stability increases with lift coefficient until a value of −0.0043 is reached at a lift coefficient of about 0.75. At this point, the trend reverses.

[redacted]

The lateral-stability parameter C_{l_ψ} increases until a value of about 0.0016 is reached at $0.6C_L$. Only a small variation is shown as lift coefficient increases further. However, an increase in Reynolds number would be expected to increase the linear range of the variation of C_{l_ψ} with C_L (reference 9). The value of C_{l_ψ} of 0.0017 at $C_L = 1.0$ indicates that the wing has considerable effective dihedral.

The data of figure 10 indicate that the characteristics in yaw at $C_L \approx 0.54$ are fairly linear to 20°, the maximum angle investigated, and that the leading-edge flaps had little effect as compared to the plain wing.

CONCLUSIONS

The results of an investigation made at low speeds to determine the aerodynamic characteristics of an airfoil-forebody swept flying-boat hull with 51.3° sweptback wing and tail indicate the following:

1. After accounting for the difference in interference effects of the support wings, the swept hull had a minimum drag coefficient about the same as the parent model or a streamline body.

2. The minimum drag coefficient for the swept hull with interference effects of the 51.3° sweptback wing was 0.0038.

3. The use of wing leading-edge flaps or leading-edge droop with fence on the wing-hull-tail combination gave a stable configuration.

4. The deflection of split or extensible split wing flaps on the wing-hull-tail combination with wing stall-control devices deflected gave a more linear variation of pitching-moment coefficient with lift coefficient; however, only the extensible split flaps were effective in increasing the maximum lift coefficient.

Langley Aeronautical Laboratory
National Advisory Committee for Aeronautics
Langley Air Force Base, Va.

[redacted]

REFERENCES

1. Yates, Campbell C., and Riebe, John M.: Effect of Length-Beam Ratio on the Aerodynamic Characteristics of Flying-Boat Hulls. NACA TN 1305, 1947.

2. Riebe, John M., and Naeseth, Rodger L.: Aerodynamic Characteristics of Three Deep-Step Planing-Tail Flying-Boat Hulls. NACA RM L8I27, 1948.

3. Riebe, John M., and Naeseth, Rodger L.: Aerodynamic Characteristics of a Refined Deep-Step Planing-Tail Flying-Boat Hull with Various Forebody and Afterbody Shapes. NACA RM L8F01, 1948.

4. McKann, Robert E., and Coffee, Claude W.: Hydrodynamic Characteristics of Aerodynamically Refined Planing-Tail Hulls. NACA RM L9B04, 1949.

5. McKann, Robert E., Coffee, Claude W., and Arabian, Donald D.: Hydrodynamic Characteristics of a Swept Planing-Tail Hull. NACA RM L9D15, 1949.

6. Foster, Gerald V., and Fitzpatrick, James E.: Longitudinal-Stability Investigation of High-Lift and Stall-Control Devices on a 52° Sweptback Wing with and without Fuselage and Horizontal Tail at a Reynolds Number of 6.8×10^6. NACA RM L8I08, 1948.

7. Koven, William, and Graham, Robert R.: Wind-Tunnel Investigation of High-Lift and Stall-Control Devices on a 37° Sweptback Wing of Aspect Ratio 6 at High Reynolds Numbers. NACA RM L8D29, 1948.

8. Lowry, John G., and Riebe, John M.: Effect of Length-Beam Ratio on Aerodynamic Characteristics of Flying-Boat Hulls without Wing Interference. NACA TN 1686, 1948.

9. Salmi, Reino J., Conner, D. William, and Graham, Robert R.: Effects of a Fuselage on the Aerodynamic Characteristics of a 42° Sweptback Wing at Reynolds Numbers to 8,000,000. NACA RM L7E13, 1947.

[redacted]

TABLE I

OFFSETS FOR LANGLEY TANK MODEL 237-68B

[All dimensions are in inches]

Station	Distance to F.P.	Keel above base line	Chine above base line	Half beam at chine	Height of hull at center line	Radius of boom	Line of centers above base line	1-inch buttock		2-inch buttock		1-inch water line	2-inch water line	3-inch water line	4-inch water line	5-inch water line	6-inch water line	7-inch water line	8-inch water line	9-inch water line	10-inch water line	11-inch water line	12-inch water line
								Upper	Lower	Upper	Lower												
F.P.	0	2.80	2.80	0	2.80																		
1	1.66	1.80	2.64	1.08	3.76			2.80	2.56				0.26	0.92									
2	4.31	.76	2.38	1.64	5.28			4.34	1.72				1.64	1.51	1.15	0.58							
3	6.96	.20	2.11	2.01	6.84			5.86	1.17	2.37	2.05		1.89	1.88	1.64	1.36	0.96						
4	9.62	0	1.84	2.24	8.35			7.44	.82	3.91	1.67		2.24	2.16	1.99	1.79	1.52	1.20	0.65				
5	12.27	0	1.60	2.36	9.72			8.78	.64	5.48	1.36		2.35	2.30	2.20	2.08	1.88	1.66	1.36	0.86			
6	14.95	0	1.34	2.41	10.80			9.92	.56	7.00	1.15		2.40	2.39	2.33	2.26	2.14	2.00	1.78	1.46	0.91		
7	17.18	0	1.14	2.34	11.52			10.72	.49	8.62	1.00		2.37	2.41	2.39	2.34	2.26	2.20	2.06	1.82	1.44	0.80	
8	20.25	0	.82	2.12	12.18			11.53	.40	9.58	.76	2.15	2.28	2.36	2.41	2.40	2.36	2.32	2.24	2.10	1.83	1.36	0.48
9	22.91	0	.58	1.73	12.56			12.04	.24	10.32	1.73	1.85	2.04	2.20	2.28	2.36	2.40	2.40	2.36	2.31	2.08	1.70	1.04
10	25.55	0	.28	1.04	12.78			12.42	.26	10.98	3.23	1.33	1.68	1.94	2.12	2.24	2.32	2.36	2.40	2.37	2.24	1.98	1.47
11¼	28.94	0	0	0	12.85			12.60	2.16	11.58	5.22	.47	.93	1.36	1.70	1.96	2.12	2.24	2.34	2.40	2.36	2.18	1.70
12	30.88	1.10			12.80			12.62	3.27	11.72	6.28		.44	.88	1.30	1.68	1.96	2.14	2.24	2.32	2.38	2.29	1.75
13	33.53	2.62			12.66			12.46	4.78	11.58	7.79			.16	.64	1.08	1.48	1.80	2.04	2.20	2.28	2.20	1.64
14	36.18	4.15			12.52	2.21	10.31		6.28	11.25	9.34					.38	.86	1.30	1.66	1.92	2.18		
15	38.84	5.68			12.39	2.08	10.31		7.82								.14	.60	1.06	1.60	2.06		
16	41.50	7.24			12.25	1.94	10.31												.31	1.40	1.92		
17	44.15				12.11	1.80	10.31																
18	46.81				11.95	1.64	10.31																
19	49.47				11.81	1.50	10.31																
20	52.13				11.68	1.37	10.31																
21	54.78				11.53	1.22	10.31																
22	57.44				11.39	1.08	10.31																
23	60.09				11.25	.94	10.31																
24	62.75				11.11	.80	10.31																
A.P.	64.34				11.02	.71	10.31																

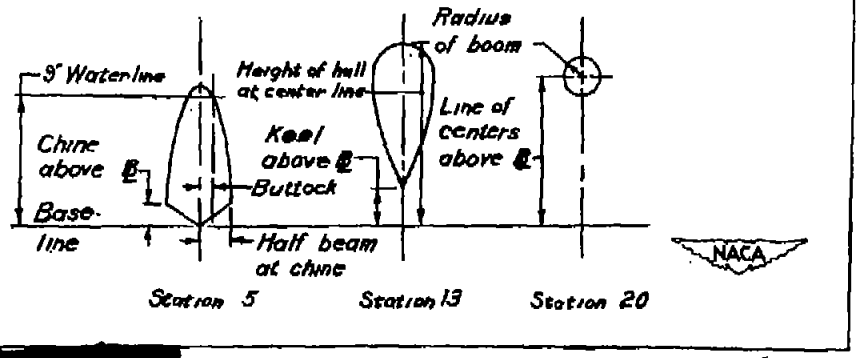

[redacted]

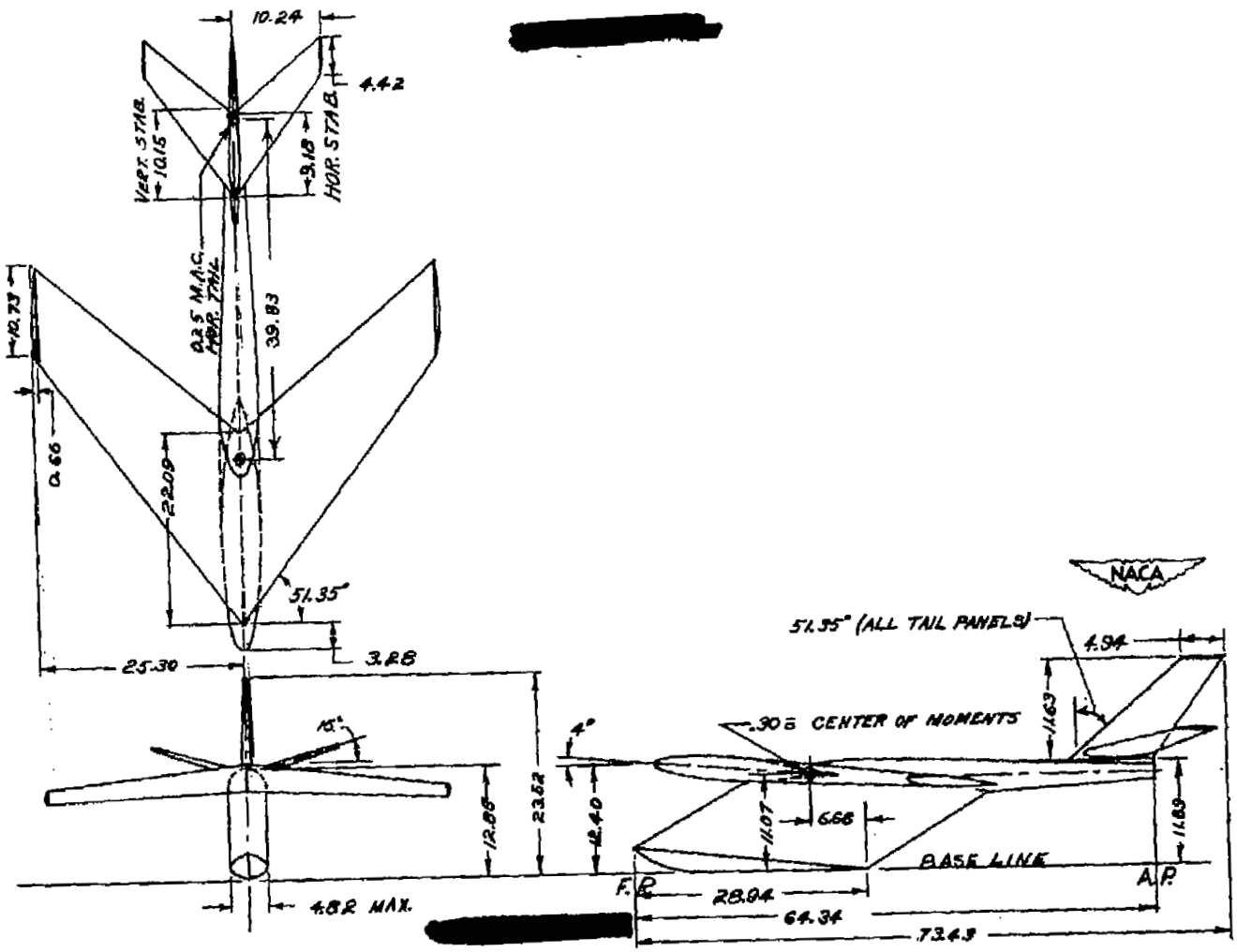

Figure 1.– Details of Langley tank model 237–68B. (All dimensions in inches.)

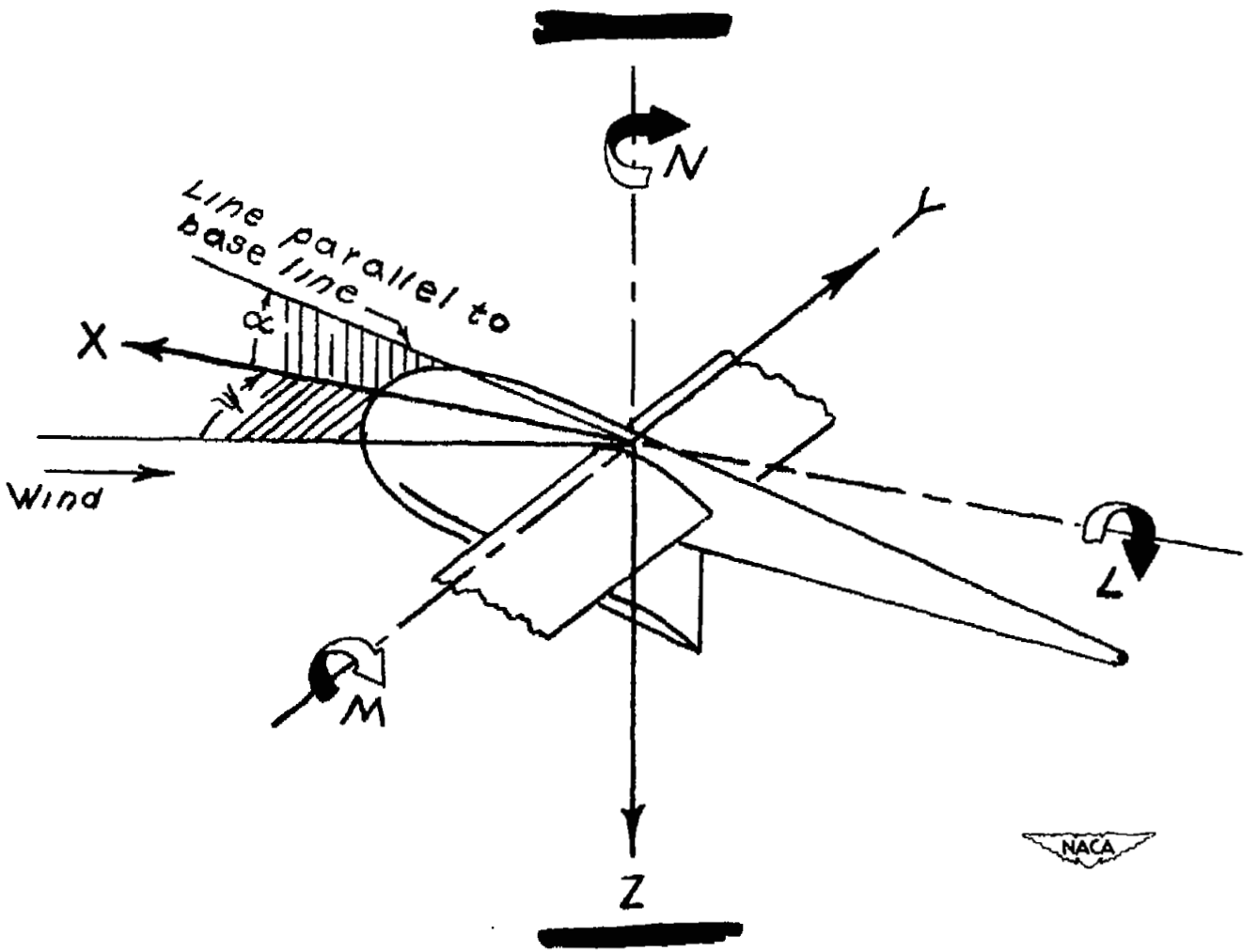

Figure 2.— System of stability axes. Positive values of forces, moments, and angles are indicated by arrows.

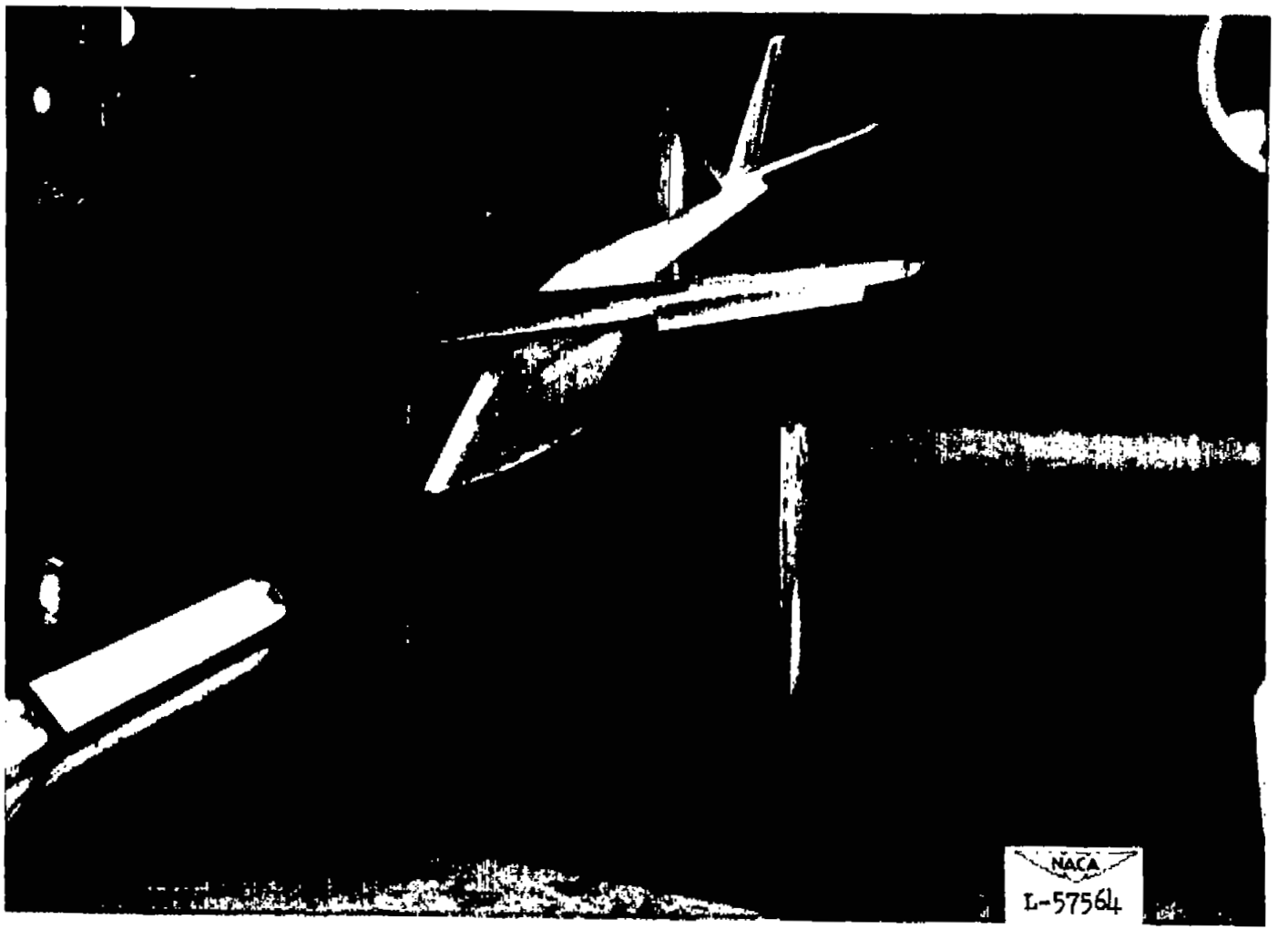

Figure 3.- Langley tank model 237-6SB mounted in the Langley 300 MPH 7- by 10-foot tunnel.

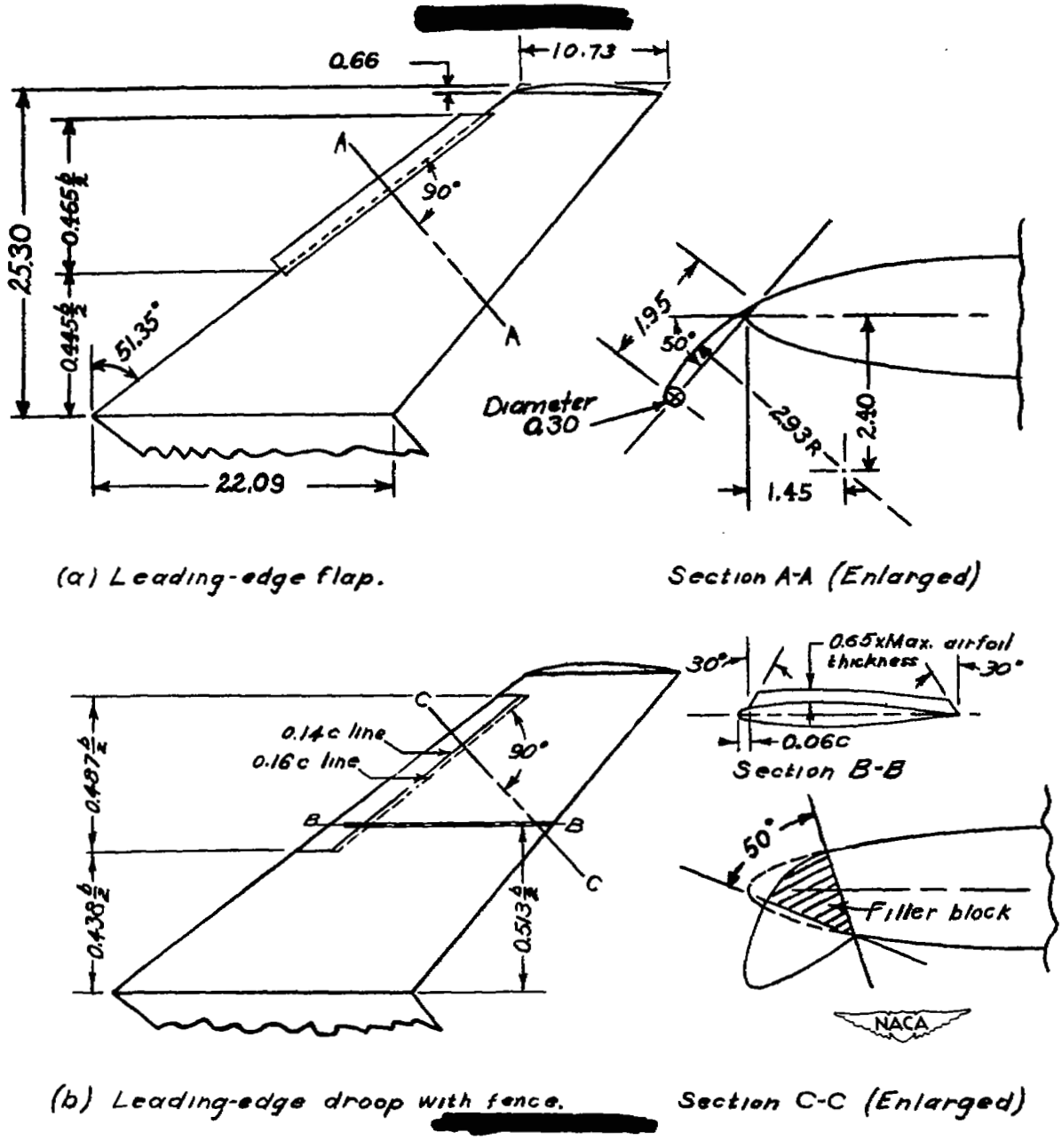

Figure 4.— Details of stall-control devices and trailing-edge flaps. (Dimensions in inches except where noted.)

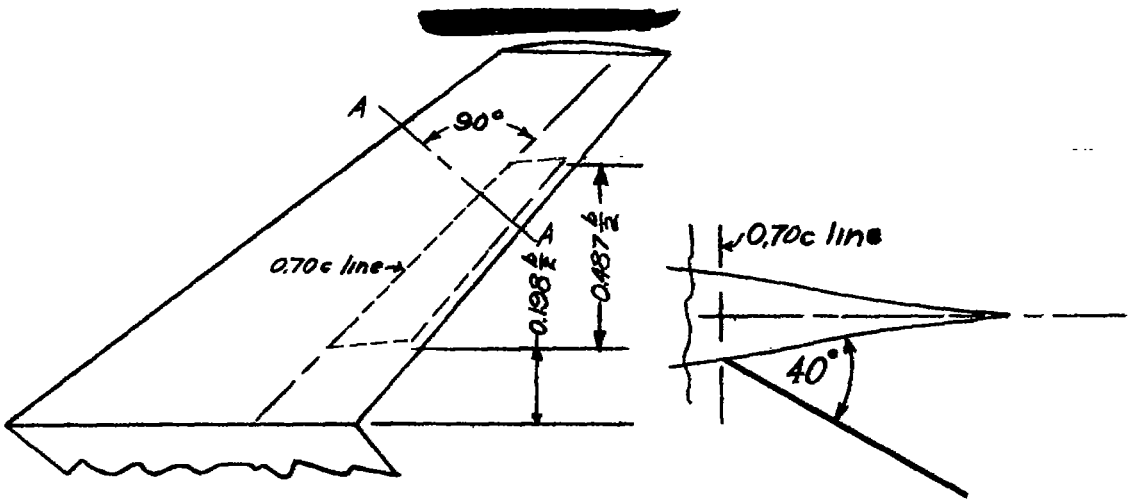

(c) Split flap. Section A-A (Enlarged)

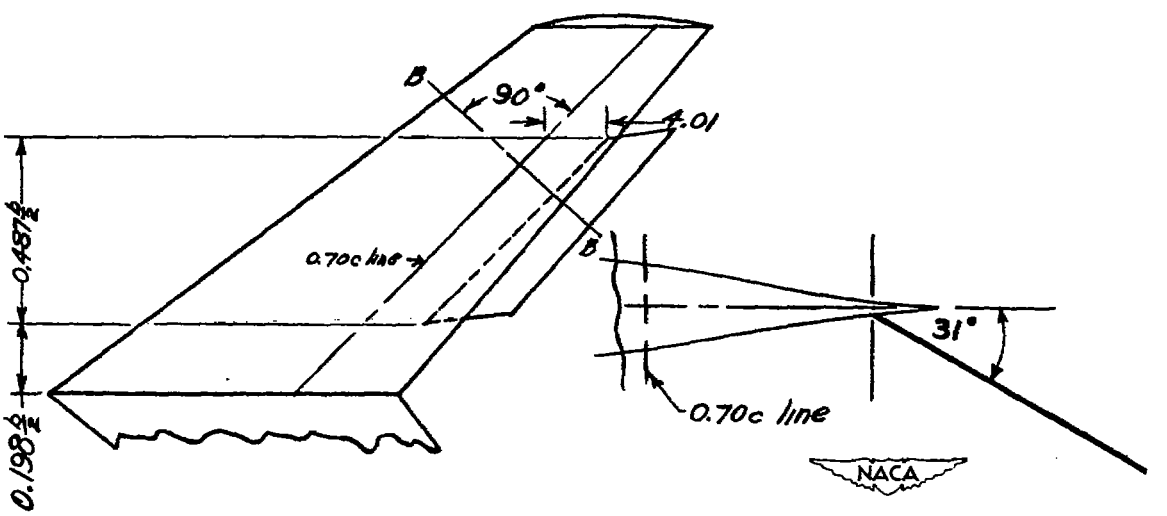

(d) Extensible split flap. Section B-B (Enlarged)

Figure 4.— Concluded.

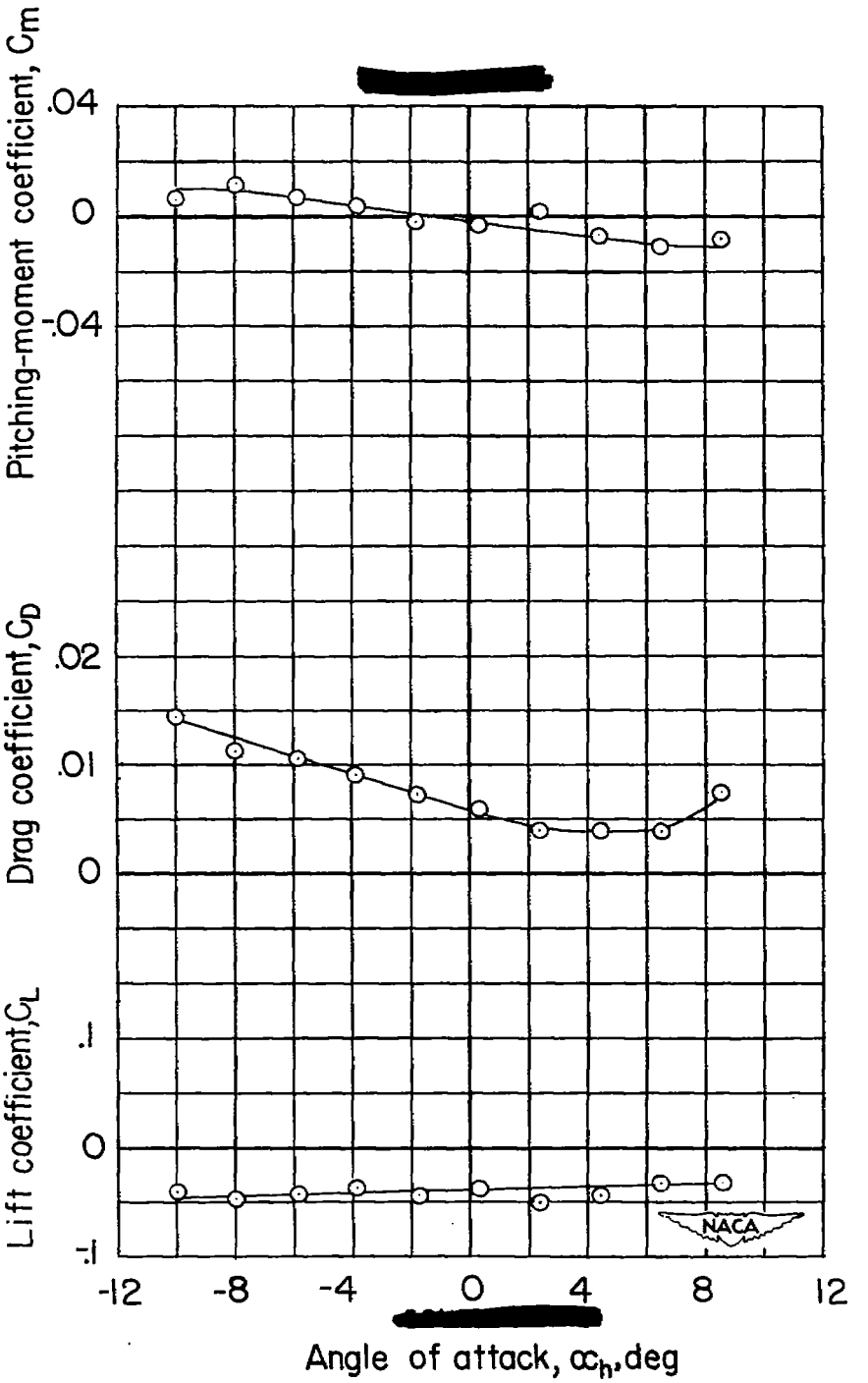

Figure 5.- Aerodynamic characteristics in pitch of Langley tank model 237-6SB with interference effects of a 51.3° sweptback wing. $R = 2.6 \times 10^6$.

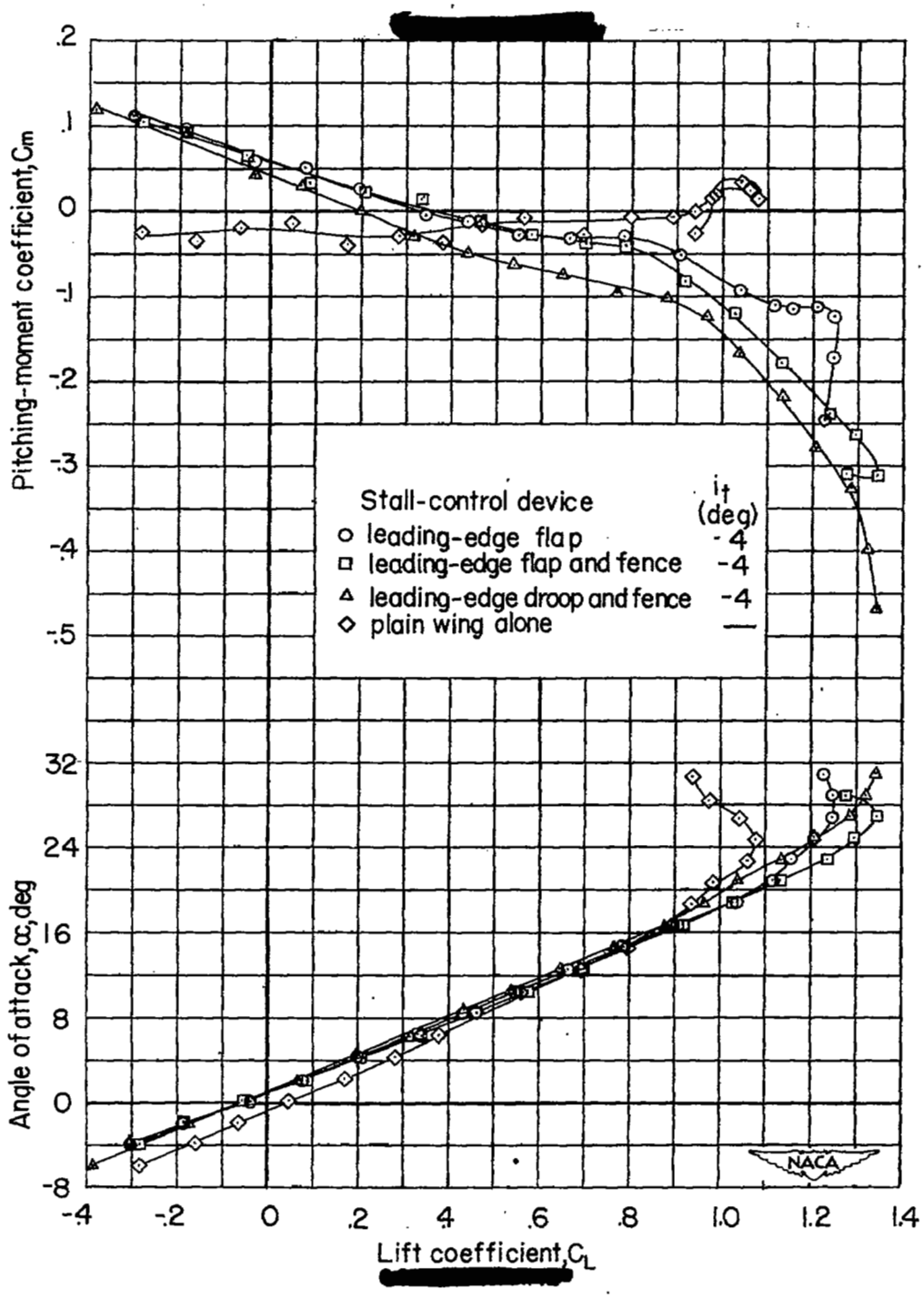

Figure 6.– Effect of leading-edge flaps and droop on the aerodynamic characteristics in pitch of Langley tank model 237-6SB with 51.3° sweptback wing and tail. Compared to the plain wing alone. $R = 0.8 \times 10^6$.

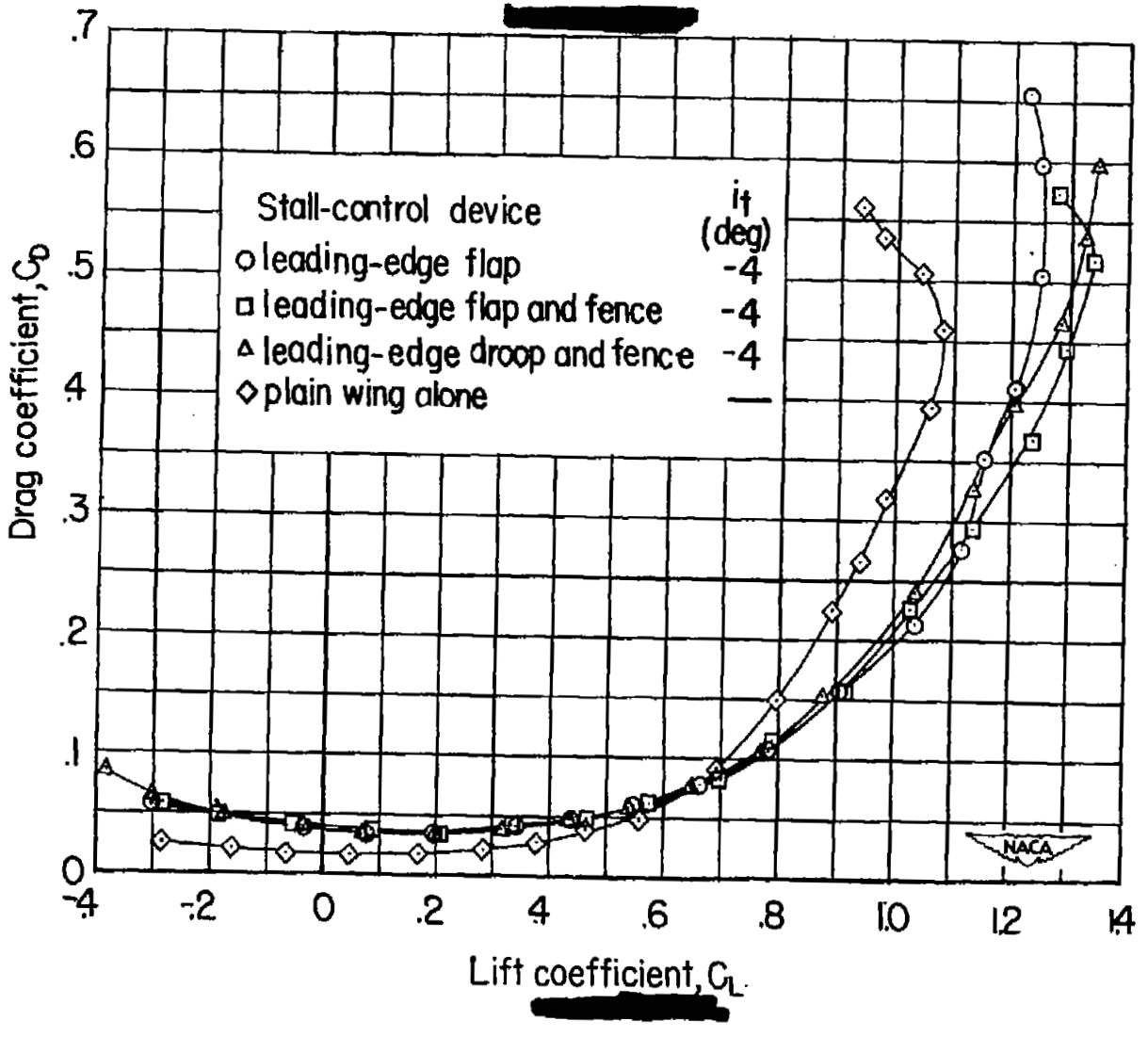

Figure 6.– Concluded.

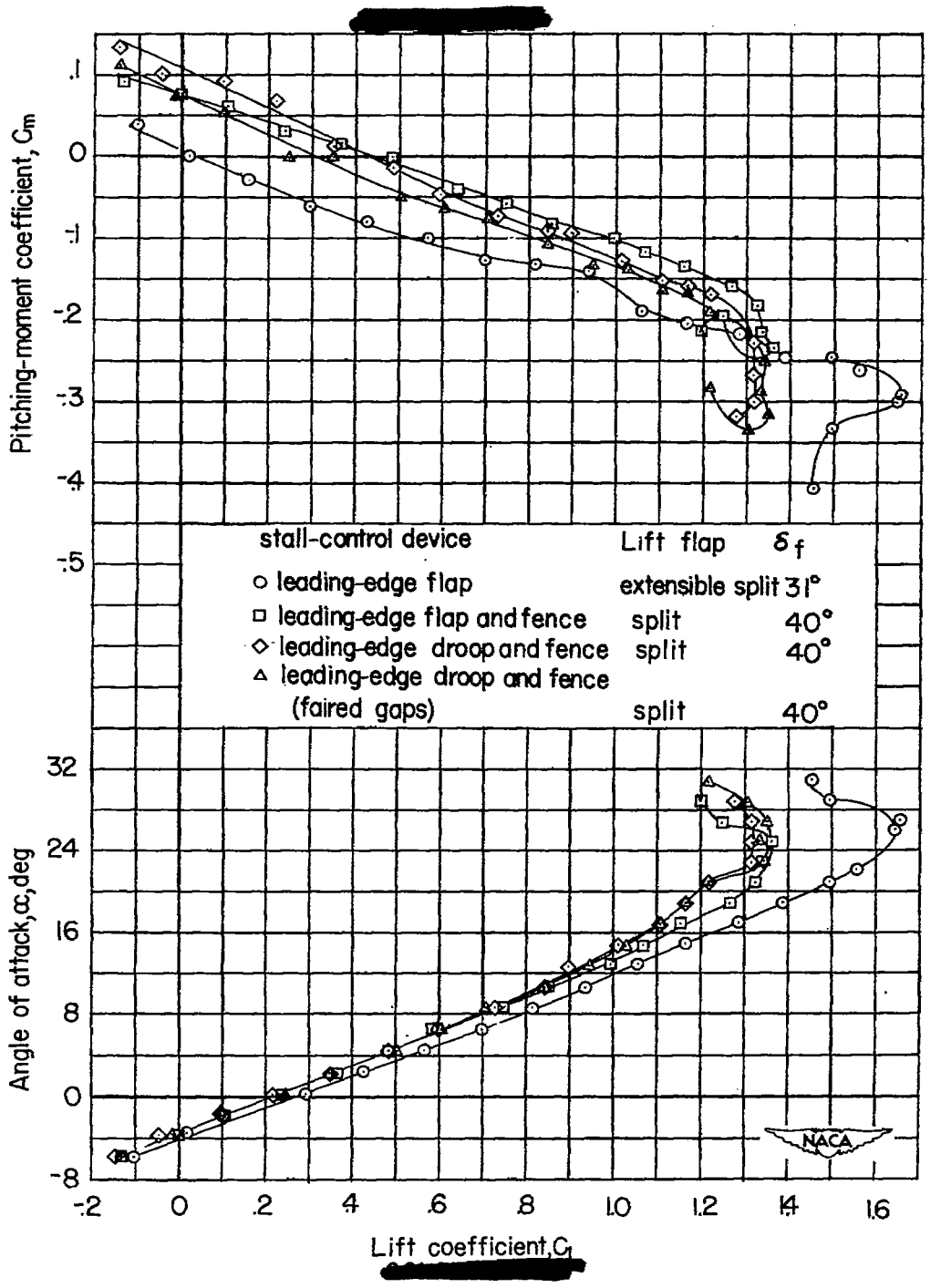

Figure 7.– Effect of lift flaps on the aerodynamic characteristics in pitch of Langley tank model 237–6SB with 51.3° sweptback wing and tail. $i_t = -4°$. Leading-edge flaps and droop wing configurations. $R = 0.8 \times 10^6$.

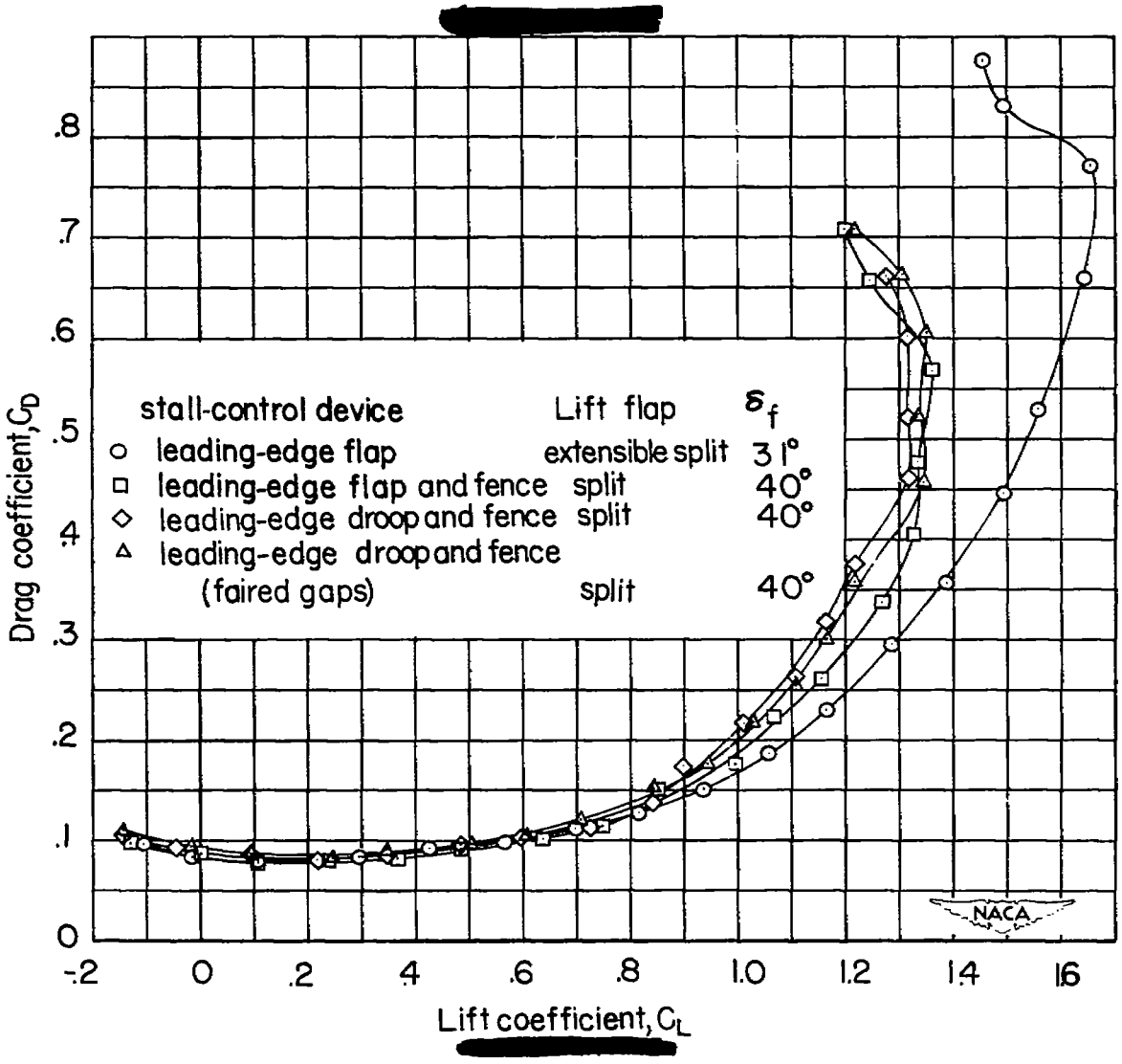

Figure 7.– Concluded.

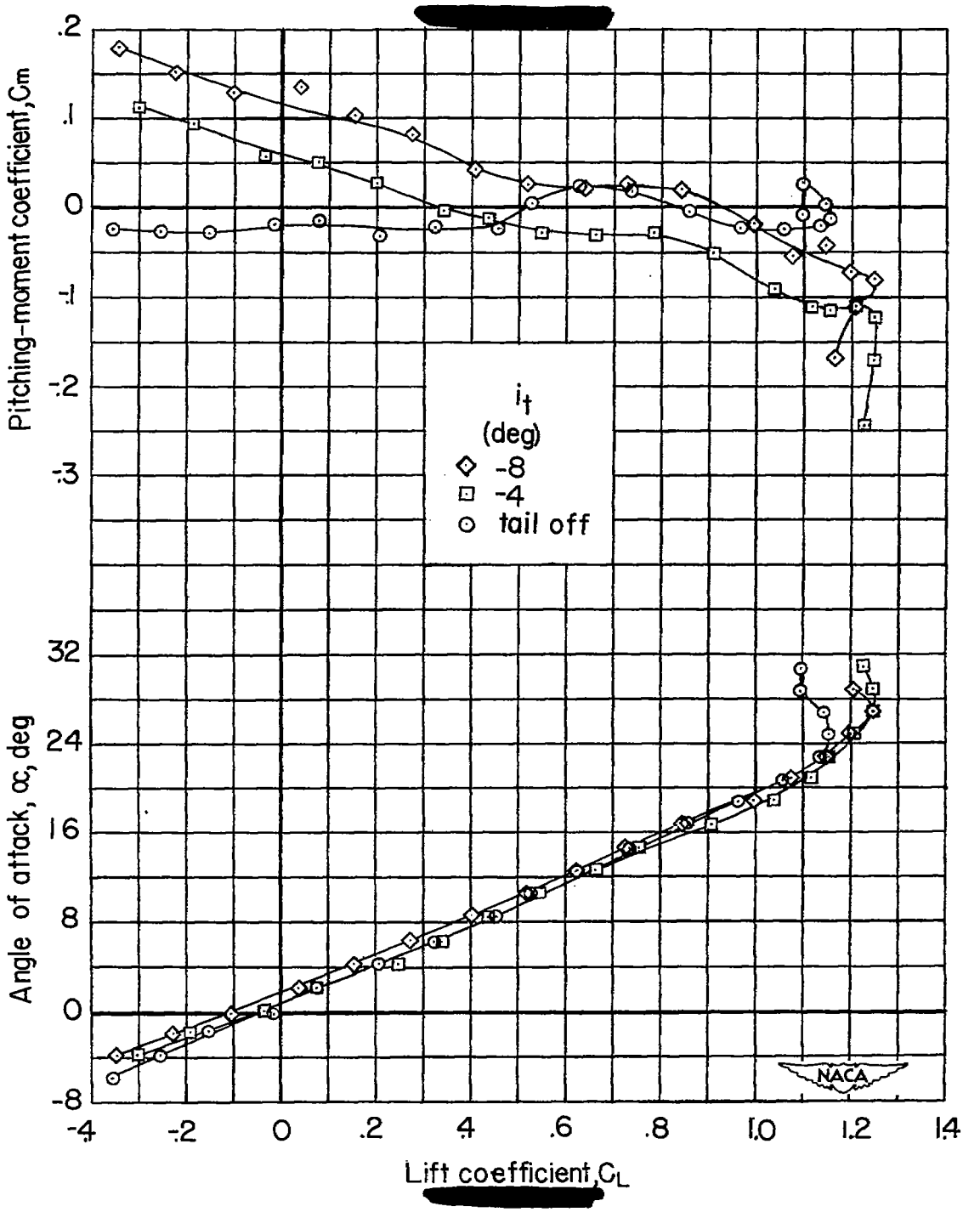

Figure 8.– Effect of tail on the aerodynamic characteristics in pitch of Langley tank model 237–6SB with 51.3° sweptback wing. Leading-edge flap deflected. $R = 0.8 \times 10^6$.

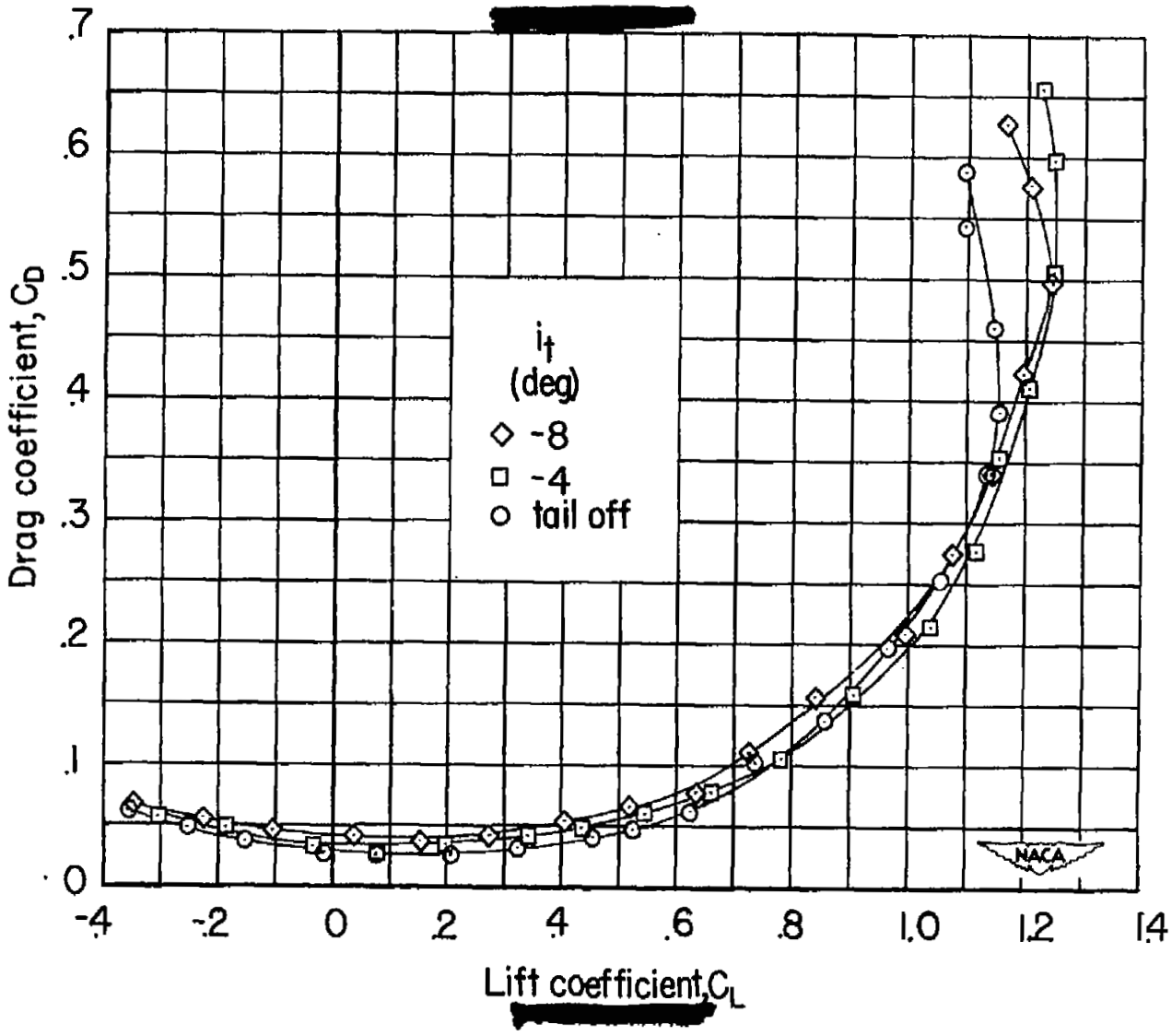

Figure 8.- Concluded.

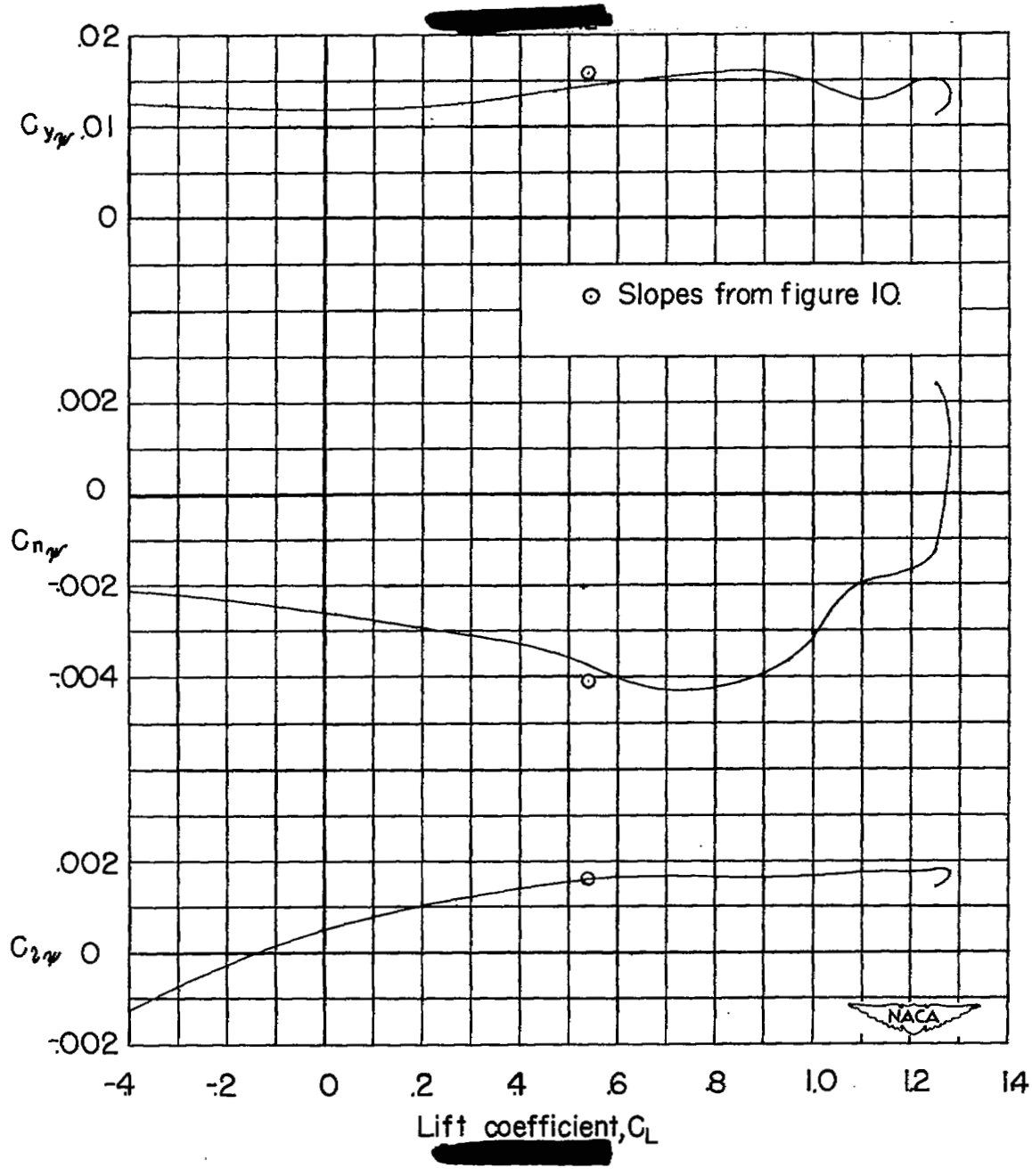

Figure 9.— Lateral-stability parameters of Langley tank model 237-68B with 51.3° sweptback wing and tail. Leading-edge flaps deflected 50°. $R = 0.8 \times 10^6$.

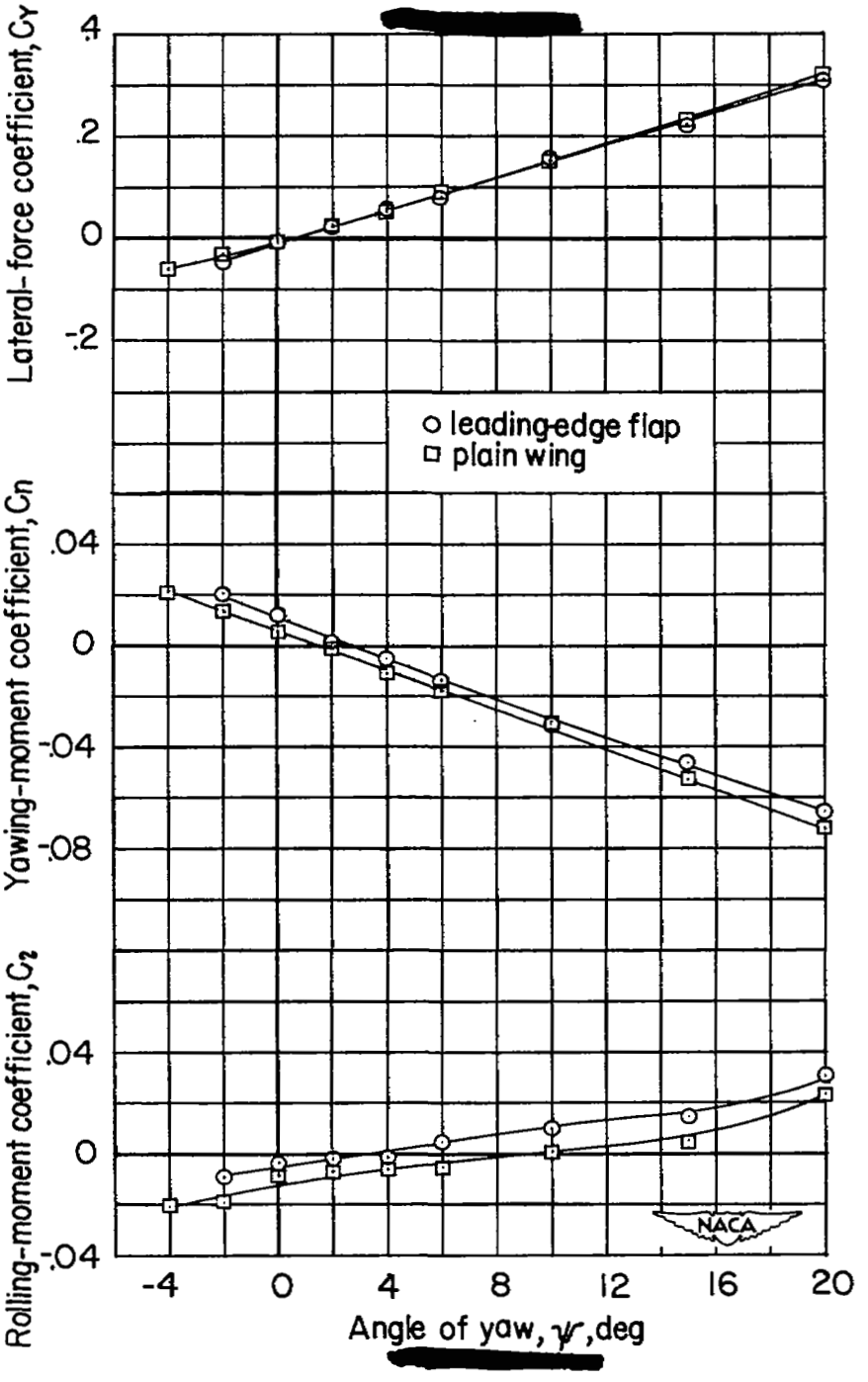

Figure 10.– Effect of leading-edge flap on the aerodynamic characteristics in yaw of Langley tank model 237–6SB with 51.3° sweptback wing and tail. $\alpha = 10.5°$, $C_L \approx 0.54$ at $\psi = 0°$. $R = 0.8 \times 10^6$.

NACA-Langley - 9-8-49 - 350